

MIDWESTERN STREAMFLOW, PRECIPITATION, AND ATMOSPHERIC VORTICITY INFLUENCED BY PACIFIC SEA-SURFACE TEMPERATURES AND TOTAL SOLAR-IRRADIANCE VARIATIONS

CHARLES A. PERRY*

U.S. Geological Survey, 4821 Quail Crest Place, Lawrence, Kansas 66049, USA

Received 11 February 2005

Revised 8 July 2005

Accepted 11 July 2005

ABSTRACT

A solar effect on streamflow in the Midwestern United States is described and supported in a six-step physical connection between total solar irradiance (TSI), tropical sea-surface temperatures (SSTs), extratropical SSTs, jet-stream vorticity, surface-layer vorticity, precipitation, and streamflow. Variations in the correlations among the individual steps indicate that the solar/hydroclimatic mechanism is complex and has a time element (lag) that may not be constant. Correct phasing, supported by consistent spectral peaks between 0.092 and 0.096 cycles per year in all data sets within the mechanism is strong evidence for its existence. A significant correlation exists between total solar irradiance and the 3-year moving average of annual streamflow for Iowa ($R = 0.67$) and for the Mississippi River at St Louis, Missouri ($R = 0.60$), during the period 1950–2000. Published in 2005 by John Wiley & Sons, Ltd.

KEY WORDS: solar-climate relations; total solar irradiance; Pacific sea-surface temperatures; atmospheric vorticity; precipitation; streamflow

1. INTRODUCTION

Streamflow produced by a basin can be utilized as an excellent indicator of climate for that basin. Streamflow is an integration of precipitation, evapotranspiration, and water storage within a watershed, parameters that are usually measured at specific locations. Storage within a basin, both in lakes and rivers or below the surface in groundwater, is usually a small fraction of the total volume of streamflow and remains fairly constant during multiyear periods. Streamflow can provide a measure of climate over large areas with relatively few data-collection sites.

The Midwestern United States (US) including Illinois, Iowa, Kansas, Minnesota, Missouri, Nebraska, South Dakota, and Wisconsin produce much of the world's supply of corn and soybeans, with Iowa producing the largest percentage. The yearly variation of climate in this region and especially Iowa has an important effect on corn and soybean production in the United States.

Most of the area of these states is drained by the Mississippi River upstream from St Louis, Missouri (U.S. Geological Survey station 07010000), which represents a drainage area of 1 805 000 km² (Figure 1). The moisture source for precipitation in this river basin is predominantly the Gulf of Mexico, which ranges from 800 to more than 2600-km distance (Hammond, 1956). Specific atmospheric flow patterns are required to move enough water vapor from the Gulf of Mexico into this area to form precipitation and create streamflow. These patterns usually require an upper-level southwesterly flow, which helps create a southerly surface-layer flow from the Gulf of Mexico. A visible decadal pattern exists in the 3-year moving average for streamflow at station 07010000 since 1950 (Figure 2). The purpose of this paper is to examine the physical processes

* Correspondence to: Charles A. Perry, U.S. Geological Survey, 4821 Quail Crest Place, Lawrence, Kansas 66049, USA; e-mail: cperry@usgs.gov

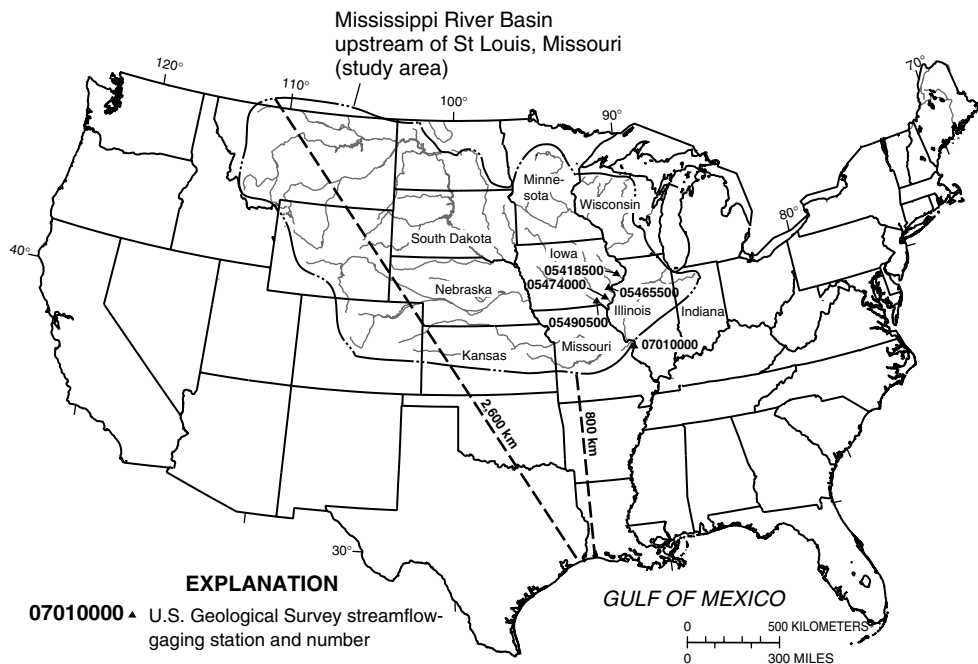


Figure 1. Map of United States showing location of study area and streamflow-gaging stations

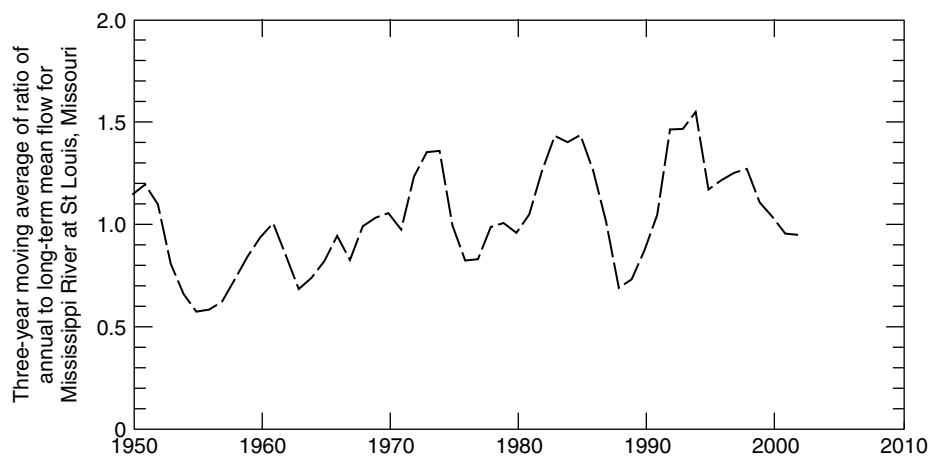


Figure 2. Graph showing 3-year moving average of the ratio of annual to long-term mean flow for Mississippi River at St Louis, Missouri, 1950–2000

that may be responsible for the variance of streamflow in Iowa and the Midwestern US and to suggest a mechanism for climatic variability.

2. PREVIOUS ANALYSES OF MIDWESTERN CLIMATE

2.1. Historical analyses

Over 150 years ago, the Midwestern US was being settled by easterners, anxious to make their fortunes farming on the sparsely populated plains. The idea that ‘rain followed the plow’ was promoted by railroad

companies and land speculators. The scientific reasoning behind the belief was that the region's atmospheric circulation was positively affected by increased sources of evaporation. This was accomplished by breaking the ground with the plow, creating open bodies of water (ponds and tanks), and planting trees whose leaves allowed the water to evaporate into the atmosphere, which ultimately returned as rain (Glantz, 1994). Only a few decades passed until the fallacy of this idea was realized. In fact, droughts came to the Midwest with a surprising regularity of approximately 22 years (Cleaveland and Duvick, 1992). Alternately, major floods occurred in 1862, 1883, 1903, 1927, 1951, 1973, and 1993 as recorded by the U.S. Geological Survey gaging station on the Mississippi River at St Louis, Missouri (station 07010000). These floods also came at approximate 22-year intervals. The 22-year climatic cycle can be teased out of proxy climate data for various areas in North America (Mitchell *et al.*, 1979). Many approximate 11-year cycles in precipitation, temperature, lake levels, river flows, and tree rings also have been observed (Hoyt and Schatten, 1997). Recently, Kodera and Kuroda (2002) demonstrated a connection between the 11-year cycle and position and intensity of stratospheric winds.

2.2. External causes of climate variability

Several external causes for these cycles have been speculated, but no physical connection has been proven. The Lunar nodal cycle of 18.6 years was an early suspect (Curie, 1981, 1984). Also, the sunspot number cycle of 10–12 years and the Hale (magnetic) sunspot cycle of 20–24 years have been suspected for years (Mitchell *et al.*, 1979). Labitzke and van Loon (1988) demonstrated the effect of the solar cycle and the quasi-biennial oscillation of the tropical stratospheric winds on the stratospheric temperatures in the northern polar atmosphere. However, other controversial results have led to much confusion over cause and effect (Hoyt and Schatten, 1997). Previously, no physical connection between magnetic properties of the sun and terrestrial climate has been unequivocally demonstrated.

Recently, the changing flux of cosmic rays has been suggested as another external cause. Cosmic rays are actually low-energy galactic charged particles whose flux varies through the solar cycle by as much as 15% (Carslaw *et al.*, 2002). Svensmark and Friis-Christensen, (1997) have argued that increased cosmic rays (during decreased solar activity and decreased solar wind speeds) tend to increase the extent of low-level clouds. According to this controversial theory, the climate would be cooler and wetter under increased low cloud cover during increases in cosmic ray flux.

The most perplexing issue for an external forcing of climate is the assumption that the effects should be observed worldwide. For example, in considering the cosmic ray theory, global cloudiness should vary directly with cosmic ray flux. However, some areas of the world have floods, some have droughts, and some have average climatic conditions, all simultaneously. If the forcing factor for climate is external, then it must be operating by regional instead of global processes.

2.3. Internal causes of climate variability

The causes of the climatic fluctuations and cycles for North America have also been postulated to have internal origins. It is well known that climate variations in certain parts of North America have close ties with the tropical Pacific Ocean temperatures associated with the El Niño/La Niña phenomena and that climatic predictions of regional streamflow are possible (Dettinger *et al.*, 1999, 2002). There is a measurable effect of El Niño/La Niña on streamflow in the upper Mississippi River Basin. Guetter and Georgakakos (1996) found above-normal streamflow in the Iowa River during El Niño and below-normal streamflow during La Niña on a seasonal basis. Nadan (1996) detected increases in precipitation during El Niño and decreases in precipitation during La Niña in Texas, Kansas, and North Dakota.

The Pacific Decadal Oscillation (PDO) (Mantua *et al.*, 1997) shows a 15–25-year fluctuation/cycle during the twentieth century, and a phase change during the mid-1970s has been associated with a step increase in streamflow characteristics in the United States (McCabe and Wolock, 2002) as well as many other Pacific Ocean and American environmental changes (Ebbesmeyer *et al.*, 1991). The Atlantic Multi-Decadal Oscillation (AMO) is an index of detrended sea-surface temperature (SST) anomalies averaged over the North Atlantic from 0–70°N and has been identified as an important mode of climate variability (Enfield *et al.*,

2001). Both the PDO and the AMO are thought to be important factors in regional multidecadal drought frequency in the United States (McCabe *et al.*, 2004).

Other indices involve atmospheric pressure such as the Pacific North American (PNA) or the North Atlantic Oscillation (NAO). The indices are nearly as numerous as the areas whose climate has been studied. A list and data links for over 30 indices can be found at: <http://www.cdc.noaa.gov/ClimateIndices/>. Interconnection between indices of ocean temperature and the resulting atmospheric responses has been described as an 'Atmospheric Bridge' (Alexander *et al.*, 2002) and has been used to explain long-distance teleconnections.

Herein lies the key to understanding North American climatic variability. North Pacific Ocean temperatures affect the atmosphere above and downwind. A study by Bond *et al.* (2003) shows that colder-than-normal SSTs throughout the eastern North Pacific Ocean and warmer SSTs northwest of Hawaii during the winters from 1999 to 2002 have altered jet-stream-level (300 hPa) wind patterns over the North Pacific and North America.

2.4. Climatic cause and effect correlations

In the past, most studies of climate variation are time-series comparisons of suspected causal phenomenon with a net climatic result. For example, an El Niño index is compared with streamflow variations in the Desert Southwest, and a certain correlation or fit is presented. However, the physical processes that are involved between SSTs and the amount of precipitation that creates the streamflow are not explained in detail. In this paper, the actual physical processes at each phase of the cause and effect are explained and supported by physical evidence in a deterministic approach.

A sequence of physically explained events is traced from observed regional streamflow that is produced by precipitation, which is generated by low-level atmospheric vorticity. Low-level vorticity, in turn, is forced by the upper atmospheric vorticity that is dictated by ocean-temperature fields. Finally, evidence for an external forcing function that explains the formation of the ocean-temperature anomalies is presented. The mechanism allows a regional response to this external forcing function (Perry, 1994, 1995, 2000).

3. DATA

3.1. Streamflow

Streamflow from four major rivers in Iowa and from the Mississippi River is used in this analysis. Annual mean discharges for four Iowa streamflow-gaging stations used as index stations for Iowa climate were obtained for the period 1950–2000 from the U.S. Geological Survey's National Water Information System (NWIS) website at <http://waterdata.usgs.gov/nwis>. These stations included the Des Moines River at Keosauqua, Iowa (station 05490500), Skunk River at Augusta, Iowa (station 05474000), Iowa River at Wapello, Iowa (station 05465500), and Maquoketa River near Maquoketa, Iowa (station 05418500) (Figure 1). These rivers represent streamflow from 57% of the area of the State of Iowa (145 765 km²). The long-term mean discharge for each gaging station was used to compute a time sequence of ratios of annual means to long-term means. These four individual time sequences were averaged, and a 3-year moving average was computed for the composite ratios. Three-year moving averages of the flow of the Mississippi River at St Louis, Missouri (station 07010000), were used to represent the total outflow from the Midwest corn- and soybean-producing area.

3.2. Precipitation

Annual precipitation from 1950 to 2000 was obtained from the National Climatic Data Center for the nine meteorological regions in Iowa. The nine regions were averaged for the state, and those values had a 3-year moving average computed.

3.3. Atmospheric vorticity

Monthly values of vorticity at the surface-layer level (0.9950 sigma) over Iowa and at the jet-stream level (0.2101 sigma) over the northern hemisphere were obtained from the Climate Diagnostic Center's National Center for Environmental Prediction (NCEP) website at <http://www.cdc.noaa.gov/cgi-bin/DataMenus.pl?stat=mon.mean&dataset=NCEP>. The gridded data set consists of values for January 1958 to November 2001 and extends around the world from 88.54°N to 88.54°S latitude. Units of vorticity are in seconds⁻¹ and at various sigma (pressure) levels. The monthly vorticity values at the two levels were converted to 3-year moving averages.

3.4. Sea-surface temperatures

Monthly mean SSTs for the North Pacific Ocean available from 1947 to 2001 were obtained from the Scripps Institute of Oceanography in La Jolla, California. The data are in a 5° grid from 130°E to 110°W longitude and from 60°N to 20°N latitude. Annual SSTs for a specified latitude/longitude range were averaged, and 3-year moving averages were computed.

3.5. Total solar irradiance

Monthly total solar-irradiance (TSI) values from 1945 to 1997 by a model developed by Lean *et al.* (1995) updated by Lean (2000), which was developed from observed TSI since 1979. The data are in watts per square meter computed at the mean Earth/Sun distance. Monthly values were converted into 3-year moving averages.

Three-year moving averages of the hydrological and meteorological data were used to smooth the annual variability. Wet and dry periods often persist longer than 12 months. The climate variability that is being investigated is working on a timescale that is longer than annual but less than decadal.

4. ANALYSES

4.1. Streamflow from precipitation

As the indexed streamflow of Iowa varies, so does the flow of the Mississippi River at St Louis, Missouri (Figure 3). Therefore, it can be assumed that the climatic conditions that affect streamflow in Iowa are quite similar to climatic conditions over much of the Midwest.

The 3-year moving average of the ratio of mean annual streamflow (annual flow to long-term mean flow) for four major rivers in Iowa, the Des Moines, Iowa, Skunk, and Maquoketa Rivers, was compared to mean annual precipitation for Iowa from 1950 to 1999 (Figure 4(A)), and as expected, the correlation is quite good ($R = 0.91$). To be significant at the 1% level with 7 degrees of freedom, the correlation coefficient must be greater than or equal to 0.40.

4.2. Precipitation from low-level vorticity

Precipitation type varies throughout the year in the form of winter snows, spring showers, and summer thunderstorms. Other than perhaps airmass-type thunderstorms, most precipitation in Iowa is produced in conjunction with surface-layer low-pressure systems. A measure of surface-layer low-pressure systems is low-level (0.9950 sigma) atmospheric vorticity. An increase in precipitation would be a result of an increase in the 0.9950-sigma vorticity, whereas a decrease in precipitation should be a result of a decrease in surface-layer vorticity. Surface-layer vorticity was computed and averaged along two lines. These lines were along 40.95°N from 95.62° to 90°W and along 91.88°W from 40.95° to 42.86°N. Figure 4(B) is a comparison between the 3-year moving average of surface-layer vorticity (0.9950 sigma) and the 3-year moving average of mean annual precipitation over Iowa from 1959 to 1999. The correlation between these data is not significant ($R = 0.37$). However, the phasing between these two factors is remarkable, especially after 1970.

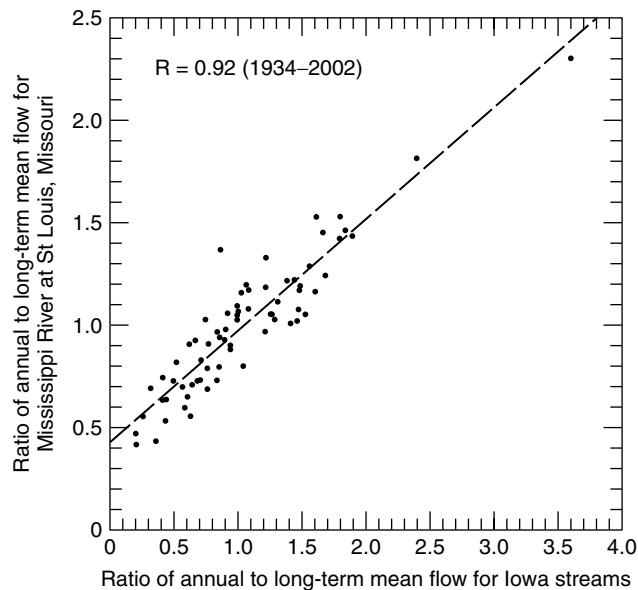


Figure 3. Graph showing correlation of ratios of annual to long-term mean flow for Mississippi River at St Louis, Missouri, and annual to long-term mean flow for Iowa streams

4.3. Low-level vorticity from jet-stream-level vorticity

Surface-layer features such as low- and high-pressure systems are controlled by the upper-level jet stream. The upper-level jet stream meanders around ridges and troughs and forms a long-wave pattern around the world in the temperate zone. This global long-wave pattern can be quite persistent with as few as three complete wavelengths in the summer to as many as six in the winter. An example of the long-wave pattern over North America is shown in Figure 5 with an average long-wave length of 75° longitude. A ridge is over the Gulf of Alaska, a trough over the western United States, and another ridge along the eastern seaboard. Through dynamic motion of the atmosphere, surface low-pressure systems generally form east of the troughs, and surface high-pressure systems form east of the ridges. Therefore, if there is a ridge in the jet-stream level over the Gulf of Alaska, there should be more surface low-pressure systems east of the upper trough over the Midwestern States. Conversely, an upper trough in the Gulf of Alaska results in more surface high-pressure systems. The jet-stream-level vorticity is calculated for a 10-by-10-degree box centered at $50^\circ\text{N } 150^\circ\text{W}$ (Area 2, Figure 6). Figure 4(C) is a comparison of the 3-year moving average of surface-layer vorticity (0.9950 sigma) over Iowa with the 3-year moving average vorticity at jet-stream level (0.2101 sigma) above Area 2 from 1959 to 1999. The correlation is significant ($R = 0.49$) for the entire period, with jet-stream ridging in Area 2 matching well with low-pressure development over Iowa (Area 3) for a 3-year moving average.

4.4. Jet-stream-level vorticity from sea-surface temperatures

The height of the pressure levels in the atmosphere is a function of the density of the air below that level. The temperature of the surface of the Earth has an effect on the density of the atmosphere above it. A warm surface will lower the density of the air, resulting in high-pressure or ridging in the upper levels near the jet stream. A cooler surface will result in more dense air and a low-pressure or troughing at altitude. As the air moves through these ridges and troughs, it turns to the right or left, depending upon the pressure field, and it speeds up or slows down. Each of these factors contributes to the vorticity field. Ridges have lower vorticity than troughs. The SST in Area 2 is compared in Figure 4(D) with the vorticity at the jet-stream level (0.2101 sigma) within the same boundaries as Area 2, and the comparison shows a significant relation ($R = 0.59$) for 1959–1998. Cool SSTs are associated with high vorticity (troughing), and warm SSTs are associated with low vorticity and ridging. (Note that vorticity increases in the negative y -direction.)

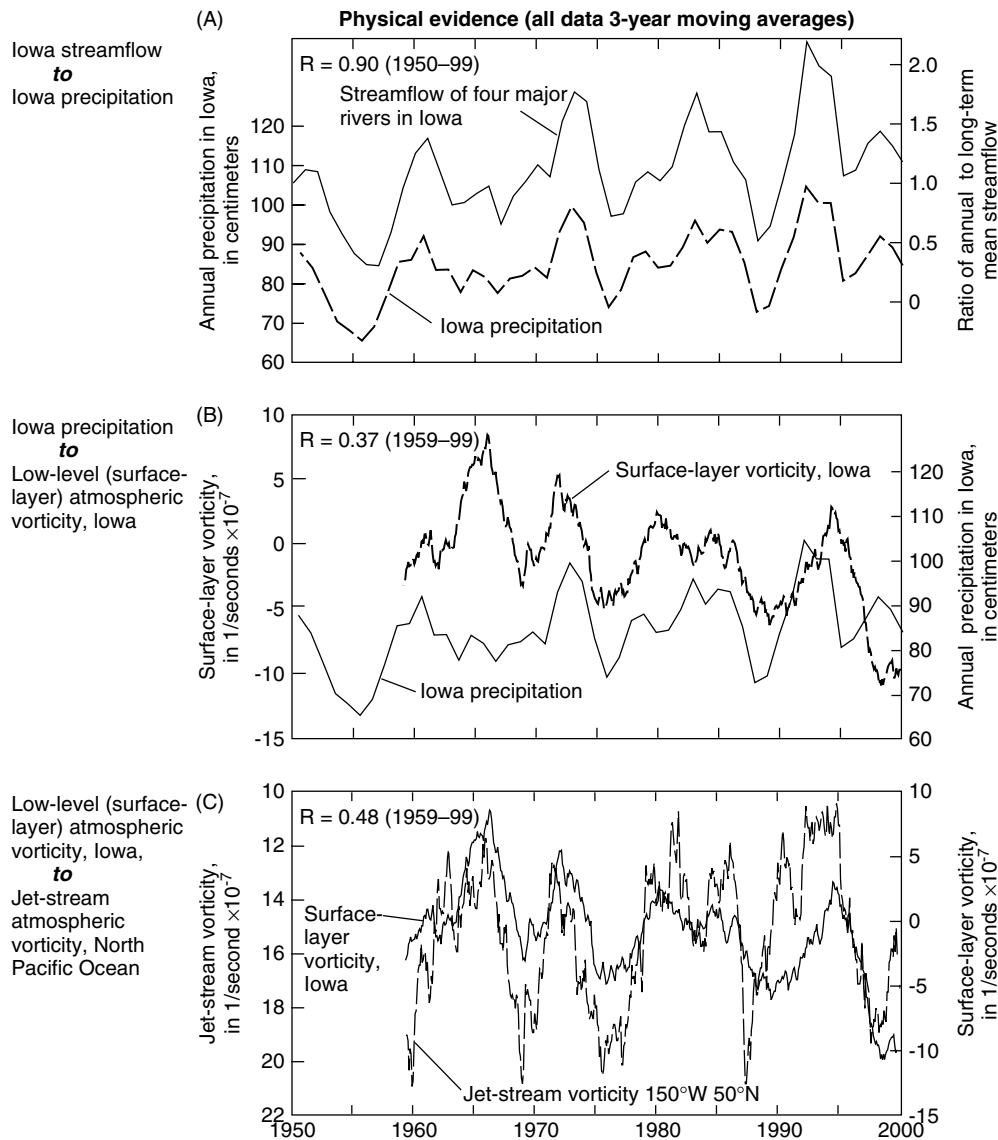


Figure 4. Graphs showing relation between 3-year moving averages of (A) Iowa streamflow and Iowa precipitation, (B) Iowa precipitation and Iowa surface-layer vorticity, (C) Iowa surface-layer vorticity and Area 2 jet-stream vorticity, (D) Area 2 jet-stream vorticity and Area 2 sea-surface temperature (SST), (E) Area 2 SST and Area 1 SST, (F) Area 1 SST and total solar irradiance

4.5. Transport of sea-surface temperature

Two major factors are responsible for the temperature of the ocean in Area 2, loss of energy to the atmosphere, and transport of energy by ocean currents. In this region of the ocean, heat is nearly always being lost to the atmosphere (Hsiung, 1985). However, the heat capacity of ocean water is many times that of the atmosphere, and so ocean temperature is slow to change. Ocean currents slowly replenish the heat by bringing warmer water from the southwestern Pacific by way of the Kuro Siwo current (analogous to the Gulf Stream in the Atlantic) and the North Pacific Drift current. If this process occurs, the temperature of Area 2 should vary in a way similar to an area in the southwestern Pacific Ocean on the north side of the Pacific Warm Pool just northeast of the Philippine Islands but with a time lag. This time lag should be the period of time for water to travel from the southwestern Pacific Ocean to the area south of the Gulf of Alaska. The

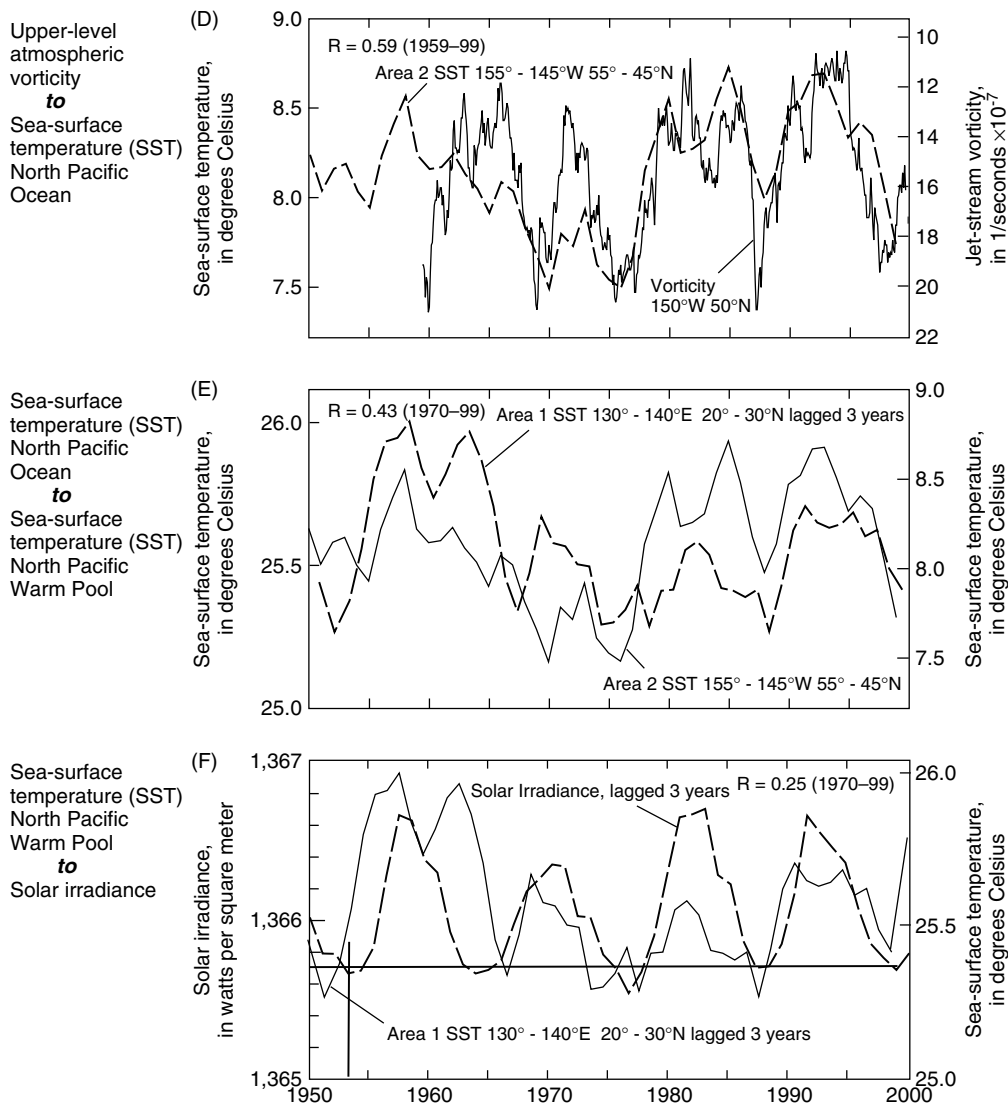


Figure 4. (Continued)

average speed of this transport could be approximately three years, the time lag that Favorite and McLain (1973) observed in the movement of a warm-temperature anomaly traveling the same course. Temperature and salinity anomalies have also been tracked over a period of several years in the Atlantic Ocean (Hansen and Bezdek, 1996). A comparison between the SST in the area $130^{\circ}-140^{\circ}\text{E}$ and $20^{\circ}-30^{\circ}\text{N}$ (Area 1) with the SST in Area 2 is significant ($R = 0.43$) from 1970 to 2000 when the SST for Area 1 is lagged three years (Figure 4(E)). The 3-year lag time gave the best correlation of the range of 0–7 years. Area 1 was chosen because it is in the northwestern part of the Pacific Warm Pool, and water from this area would most likely be drawn into the Kuro Siwo current.

4.6. Sea-surface temperatures from total solar irradiance

The origins of the SST anomalies in the western tropical Pacific Ocean are subtle and complex. However, the basic fact remains that the ocean acquires energy in the tropics and transports it northward. One method of acquiring energy is through the absorption of radiant energy from the Sun.

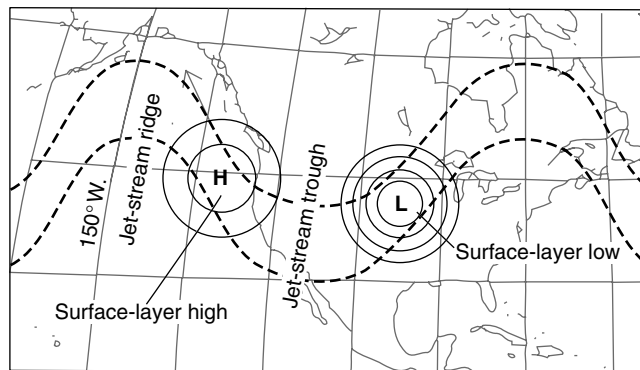


Figure 5. Map showing relation between jet-stream ridges and troughs and surface-layer high- and low-pressure systems

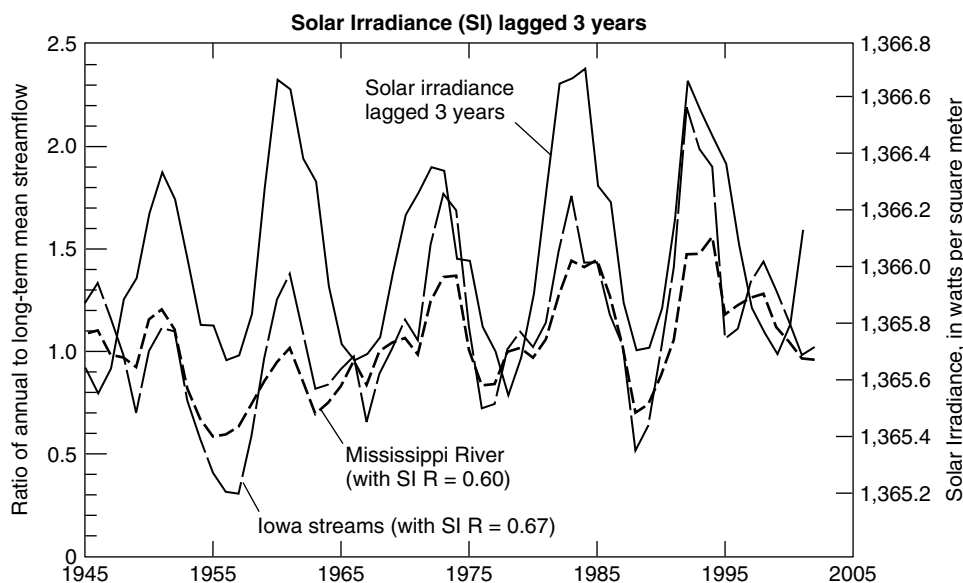


Figure 6. Graph showing relation between total solar irradiance and streamflow in Iowa and the Mississippi River at St Louis

Although SSTs show significant coupling with atmospheric parameters (Wallace *et al.*, 1990), it is not the ocean's surface that stores the majority of the solar energy. The visible spectrum contains about one-half of the total energy available from the Sun at the Earth's surface (Liov, 1980), and those wavelengths can penetrate well below the ocean's surface. Lewis *et al.* (1990) showed that solar radiation in visible frequencies, usually assumed to be absorbed at the sea surface, penetrates to a substantial depth below the upper mixed layer of the ocean that interacts directly with the atmosphere.

The transparency of the tropical oceans is dependent upon the amount of biogenic material, phytoplankton pigments, and the degradation products that are present. In the Pacific Ocean, transparency increases from east to west, with greatest penetration of solar energy occurring in the western tropical Pacific. The net radiative transport of heat downward through the base of the mixed layer (which varies from 10 m in the eastern and western Pacific to about 60 m in the central Pacific) is approximately equivalent to the estimated climatological net surface-heat flux into the ocean over much of the western Pacific (Lewis *et al.*, 1990). This heat returns to the ocean's surface months or years later to interact with the atmosphere as the general circulation of the Pacific Gyre transports the water northward and eastward toward North America.

If there is a variation in the amount of radiant energy received by the ocean, then the energy stored within the ocean should vary in a similar manner. Significant correlations exist between TSI and ocean-temperature data (White *et al.*, 1998). TSI flux was compared with the tropical SSTs in the western Pacific Ocean in Area 1 in Figure 4(F). If TSI flux is high, then there should be warmer SSTs as a result of increased energy. The graph does show a connection between the TSI and SST data from 1970 to 2000 with a 0-year lag time. Although the amplitudes of the two time series are not consistent, resulting in a less than significant agreement ($R = 0.25$), the phasing is in good agreement. The comparison is noteworthy because the El Niño/La Niña effect is quite strong in this region.

4.7. Consistent phasing of supporting time-series data

Even though the progression of physical connections between streamflow, precipitation, low-level vorticity, jet-stream vorticity, SST in the Gulf of Alaska, SST in the north part of the Pacific Warm Pool, and TSI have a range in correlation coefficients from a significant $R = 0.90$ to an insignificant $R = 0.25$, the phasing between each of the data sets is consistent. A measure of the degree of phasing of the data sets is a comparison of the spectrum analysis for each data set used in the correlations. All data sets demonstrated significant spectral power in the range of frequency from 0.092 to 0.096 cycles per year (10.8 to 10.4 year cycles).

With lower correlation coefficients for some of the steps in the six-step sequence of physical connections, a correlation between TSI (cause) and streamflow (effect) would be expected to be negligible. However, the comparison between Iowa-indexed streamflow and TSI variations is comparatively quite high (Figure 6) with $R = 0.67$. This final correlation is an indication that although the intermediate areas chosen for this study may not be the most influential areas or the location of the influential areas may be moving in time, the relation between TSI and streamflow in Iowa is significant and can explain 45% of the Iowa streamflow variability.

As shown in Figure 3, the indexed flow of the four Iowa rivers is representative of the flow of the Mississippi River at St Louis, Missouri. Streamflow records at this gage (station 07010000) also show a good relation with TSI ($R = 0.60$). Climatic conditions and the factors that effect Iowa streamflow are similar to those of the other Midwestern states.

5. DISCUSSION

By taking the deterministic approach of stepping through the individual physical processes involved, TSI variations can be a plausible cause of climatic variations in the upper Mississippi River Basin. A solar/hydroclimatic mechanism that accounts for each physical process (Figure 7) can be described.

The mechanism begins with the absorption of varying amounts of solar energy into the tropical Pacific Ocean Warm Pool, creating ocean-temperature anomalies (step 1). The ocean-temperature anomalies then are transported over time (approximately 3 years) by ocean currents from the southwestern Pacific Ocean to the North Pacific Ocean (step 2) where the warmer or colder-than-normal water initiates the development of ridges or troughs in the upper atmosphere at jet-stream levels (step 3). Upper atmospheric ridges or troughs in the North Pacific have a distinct effect on the formation of lower atmospheric low-pressure or high-pressure systems over North America (step 4). Low-pressure systems produce precipitation (step 5), and their intensity and frequency determine the regional hydrologic response of streamflow (step 6).

The location, strength, and wavelength of the jet stream help determine what part of North America is wet or dry. Even though the TSI variations are global, the solar/hydroclimatic mechanism presented here allows for regional variability through the creation and movement of ocean-temperature anomalies.

The variability of Midwestern streamflow explained by TSI from 1950 to 2000 accounts for almost one-half of the total (45%). The time lag is not constant during this 50-year period with the first two decades having about a 4-year lag. The variation in time lag could be a function of ocean current velocities. Other factors such as El Niño/La Niña (NINO3 index, 1950–2000) have some influence on streamflow in the Midwest but can only account for less than 10% of the variability of Iowa streamflow on an annual basis and less than 1% on a 3-year moving average comparison. There also would be an effect of Atlantic Ocean SSTs on the

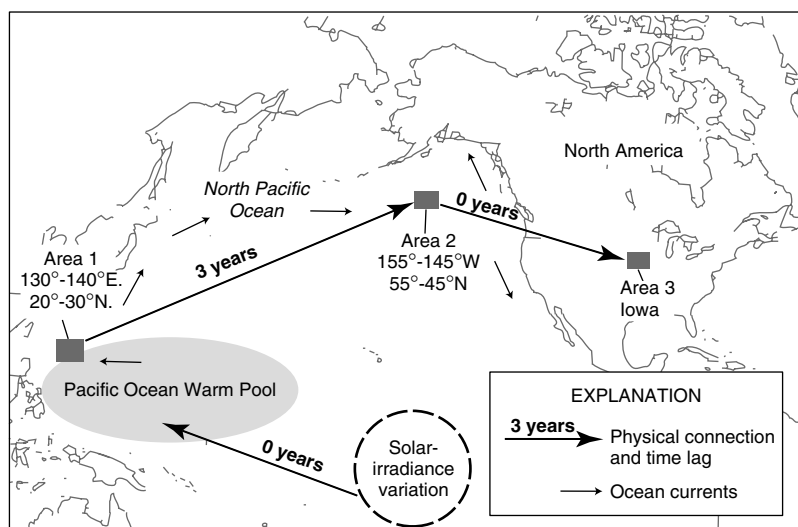


Figure 7. Schematic of solar/hydroclimatic mechanism

development of upper-level vorticity over North America. However, on the basis of the results presented in this paper, TSI effects on Pacific Ocean temperatures and vorticity patterns have a viable connection with streamflow in the central part of North America.

6. SUMMARY

A six-step mechanism for a solar/climate connection for the Midwestern United States in central North America was examined in this paper. A 50-year sequence of annual TSI was correlated with SSTs just northeast of the Philippine Islands in the area 130° to 140°E and 20° to 30°N (Area 1). Next, the SSTs in Area 1 were correlated with SSTs in the eastern North Pacific Ocean at 150°W and 50°N (Area 2). The correlation shows a 3-year lag, long enough to allow for transport of SST anomalies by ocean currents. Then, the SSTs in Area 2 are correlated with the vorticity above Area 2 at the jet-stream level, which provides a measure of upper atmospheric ridging or troughing. Warmer SSTs initiate the development of ridges (lower vorticity), and the cooler SSTs initiate the development of troughs (higher vorticity). Subsequently, upper atmospheric ridges near Area 2 tend to form lower atmospheric low-pressure systems over Iowa and central North America, and, conversely, troughs form high-pressure systems. The upper atmospheric vorticity over Area 2 is correlated with the lower atmospheric vorticity over Iowa. Finally, the lower atmospheric vorticity over Iowa is correlated with average Iowa precipitation and with a mean ratio of annual flow to long-term mean flow for four major rivers in Iowa.

Even though the correlation coefficients are not always above the level of significance, consistent phasing of the climate linkages to the solar forcing is strong evidence for its existence. The correlation between the original TSI signal, lagged 3 years, and the long-term mean flow for Iowa rivers is significant ($R = 0.67$). The relation between TSI and Midwest streamflow is also evident in the fact that the flow of the Mississippi River at St Louis, Missouri, shows a significant relation with TSI ($R = 0.60$).

REFERENCES

- Alexander MA, Blade I, Newman M, Lanzante JR, Lau N-C, Scott JD. 2002. The atmospheric bridge: the influence of ENSO teleconnections on air-sea interaction over the global oceans. *Journal of Climate* **15**: 2205–2231.
 Bond NA, Overland JE, Spillman M, Stabeno P. 2003. Recent shifts in the state of the North Pacific. *Geophysical Research Letters* **30**: 2183.
 Carslaw KS, Harrison RG, Kirkby J. 2002. Cosmic rays, clouds, and climate. *Science* **298**: 1732–1737.

- Cleaveland MK, Duvick DN. 1992. Iowa climate reconstructed from tree rings, 1640–1982. *Water Resources Research* **28**: 2607–2615.
- Curie RG. 1981. Evidence for 18.6-year signal in temperature and drought conditions in North America since AD 1800. *Journal of Geophysical Research* **86**: 11 055–11 064.
- Curie RG. 1984. Evidence for 18.6-year lunar nodal drought in western North America during the last millennium. *Journal of Geophysical Research* **89**: 1295–1308.
- Dettinger MD, Cayan DR, Redmond KT. 1999. United States streamflow probabilities based on forecasted La Niña, winter-spring 2000. *Experimental Long-Lead Forecast Bulletin* **8**: 57–61.
- Dettinger MD, Cayan DR, Redmond KT. 2002. United States streamflow probabilities and uncertainties based on anticipated El Niño, water year 2003. *Experimental Long-Lead Forecast Bulletin* **11**: 46–52.
- Ebbesmeyer CC, Cayan DR, McClain DR, Nichols FH, Peterson DH, Redmond KT. 1991. 1976 step in Pacific climate: forty environmental changes between 1968–1975 and 1977–1984. In *Proceedings of the 7th Annual Pacific Climate (PACCLIM) Workshop*, Betancourt JL, Tharp VL (eds). California Department of Water Resources: Interagency Ecological Study Program Technical Report 26, Sacramento, California, 115–126.
- Enfield DB, Mestas-Nunez AM, Trimble PJ. 2001. The Atlantic multidecadal oscillation and its relationship to rainfall and river flows in the continental U.S. *Geophysical Research Letters* **28**: 277–280.
- Favorite F, McLain DR. 1973. Coherence in transpacific movements of positive and negative anomalies of sea surface temperature. *Nature* **244**: 139–143.
- Glantz MH. 1994. *Drought Follows the Plow*. Cambridge University Press: Cambridge.
- Guetter AK, Georgakakos KP. 1996. Are the El Niño and La Niña predictors of Iowa river seasonal flow? *Journal of Applied Meteorology* **35**: 690–705.
- Hammond CS. 1956. *Hammond's Ambassador World Atlas*. CS Hammond & Company: New York.
- Hansen DV, Bezdek HF. 1996. On the nature of decadal anomalies in North Atlantic sea surface temperature. *Journal of Geophysical Research* **101**: 8749–8758.
- Hsiung J. 1985. Estimates of global oceanic meridional heat transport. *Journal of Physical Oceanography* **15**: 1405–1413.
- Hoyt DV, Schatten KH. 1997. *The Role of the Sun in Climate Change*. Oxford University Press: Oxford.
- Kodera K, Kuroda Y. 2002. Dynamical response to the solar cycle. *Journal of Geophysical Research* **107**: 4749.
- Labitze K, van Loon H. 1988. Associations between the 11-year solar cycle, the quasi-biennial oscillation and the atmosphere part I, the troposphere and stratosphere in the northern hemisphere in winter. *Journal Atmospheric and Terrestrial Physics* **50**: 197–206.
- Lean J, Beer J, Bradley R. 1995. Reconstruction of solar irradiance since 1600. *Geophysical Research Letters* **22**: 3195–3198.
- Lean Judith. 2000. Evolution of the Sun's spectral irradiance since the Maunder Minimum. *Geophysical Research Letters* **27**: 2425–2428.
- Lewis MR, Carr M, Feldman GC, Esaias W, McClain C. 1990. Influence of penetrating solar radiation on the heat budget of the equatorial Pacific Ocean. *Nature* **347**: 543–545.
- Liov KN. 1980. *An Introduction to Atmospheric Radiation*. Academic Press: New York.
- Mantua NJ, Hare SR, Zhang Y, Wallace JM, Francis RC. 1997. A Pacific interdecadal climate oscillation with impacts on salmon production. *Bulletin American Meteorological Society* **78**: 1069–1079.
- McCabe GJ, Wolock DM. 2002. A step increase in streamflow in the conterminous United States. *Geophysical Research Letters* **29**: 2185.
- McCabe GJ, Palecki MA, Betancourt JL. 2004. Pacific and Atlantic Ocean influences on multidecadal drought frequency in the United States. *Proceedings National Academy Science* **101**: 4136–4141.
- Mitchell JM Jr, Stockton CW, Meko DM. 1979. Evidence of a 22-year rhythm of drought in the western United States related to the Hale solar cycle since the 17th century. In *Solar-Terrestrial Influence on Weather and Climate*, McCormac BM, Seliga TA (eds). D. Reidel: Dordrecht, 125–143.
- Nadan RJ. 1996. The ENSO cycle associated with united states Midwest precipitation, Masters Thesis, Kansas University.
- Perry CA. 1994. Solar-irradiance variations and regional precipitation fluctuations in the western United States. *International Journal of Climatology* **14**: 969–983.
- Perry CA. 1995. Association between solar-irradiance variations and hydroclimatology of selected regions of the USA. In *Proceedings of 6th International Meeting on Statistical Climatology*. Galway, 239–242.
- Perry CA. 2000. A regression model for annual streamflow in the Upper Mississippi River Basin based on total solar irradiance. In *Proceedings of the Sixteenth Annual Pacific Climate Workshop*, West GJ, Buffaloe LD (eds). Interagency Ecological Program for Sacramento-San Joaquin Delta: Technical Report 65, Sacramento, California, 161–170.
- Svensmark J, Friis-Christensen E. 1997. Variation of cosmic ray flux and global cloud coverage – a missing link in solar-climate relationships. *Journal Atmospheric Solar-Terrestrial Physics* **59**: 1225–1232.
- Wallace JM, Smith C, Jiang Q. 1990. Spatial patterns of atmosphere-ocean interaction in the northern winter. *Journal of Climate* **3**: 990–998.
- White WB, Cayan DR, Lean J. 1998. Global upper ocean heat storage response to radiative forcing from changing solar irradiance and increasing greenhouse gas/aerosol concentrations. *Journal Geophysical Research* **103**: 21 355–21 366.